

Finite-Energy Sum Rules for Five-Point Amplitudes

S. Humble

Daresbury Nuclear Physics Laboratory, Daresbury, Near Warrington, Lancashire, England

(Received 7 February 1972)

Finite-energy sum rules (FESR's) for single-particle production amplitudes are derived by considering the analytic structure of all orders of Feynman diagrams. Keeping only the bound-state pole terms in the sum rules, the suppression of exotic exchanges leads to the relation for the πN scattering lengths, $2a_{3/2} + a_{1/2} \approx 0$. A preliminary partial-wave analysis of the low-energy production data is also described. The results of this analysis in the FESR's strongly support the hypothesis of duality for production processes.

I. INTRODUCTION

The dispersion-relation approach to two-body hadron physics has had many successes in the past decade, not the least of which has been in the formulation of finite-energy sum rules (FESR's) and their definition of "duality."¹ However, until now there has been no similar practical dispersion-relation approach for production processes, and consequently the interpretation of duality for production amplitudes has rested solely on the formulation of mathematical models. Much work has recently been done in trying to fit these models to the data, but the problems inherent in this approach make the results, at best, inconclusive.² It is clear that there is a general discrepancy between the model predictions and the experimental results, but the reasons are not understood. There are numerous approximations made in the fits, such as an almost total disregard for the spin structure of the production amplitudes and an arbitrary extrapolation to finite resonance widths. However, it is also possible that the discrepancy is more fundamental and is a consequence of the dual models themselves. For this reason we derive in this paper FESR's for five-point amplitudes in which it is possible to examine the experimental information more closely and to test whether the data (or rather accepted model fits to the data) satisfy the resulting definition of duality for production processes.

One of the main advantages of the FESR's of course is that they are written in terms of amplitudes rather than spin-averaged cross sections. Thus they can provide sensitive tests of various high-energy models. However, to do this one needs very detailed knowledge of the low-energy amplitude, which is not yet available for single-particle production processes. Indeed without polarization measurements we have to rely on assuming dominance of the production amplitude by

a few well-known resonances. Nevertheless from the preliminary investigation of the FESR presented in this paper it is clear that even this approximate treatment of the low-energy amplitudes is sufficient to provide an interesting insight into the structure of the high-energy amplitudes. Furthermore, as we shall indicate later, the FESR's themselves may be very valuable in helping to determine the low-energy partial waves.

The outline of the paper is as follows. In the next two sections we discuss some of the difficulties associated with writing dispersion relations for production amplitudes and indicate how these can be overcome to construct our finite-energy sum rules. In Sec. IV we show how these sum rules can be used, keeping only the bound-state pole terms for the process $\pi N \rightarrow \pi\pi N$, to provide an interesting condition on the low-energy πN amplitudes. We conclude, in the last two sections, with an account of a preliminary production partial-wave analysis we have performed and its implications via the FESR's for the high-energy amplitudes.

II. ANALYTICITY CONSIDERATIONS FOR THE FIVE-POINT AMPLITUDE

Before discussing the derivation of our dispersion relations and FESR's for five-point amplitudes, it is perhaps instructive to outline briefly some of the difficulties inherent in this approach. For the most part these difficulties arise because of the increased number of variables in the problem, which complicates the analytic structure of the production amplitude. For instance for the single-particle production process shown in Fig. 1, besides the particle masses, we can construct ten Lorentz scalars from the various four momenta which we denote by

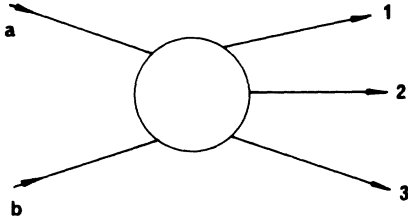


FIG. 1. Five-point amplitude.

$$\begin{aligned}
 s &= (p_1 + p_2)^2, \\
 s_i &= (q_j + q_k)^2, \quad i \neq j \neq k = 1, 2, 3 \\
 t_i &= (p_a - q_i)^2, \quad i = 1, 2, 3 \\
 u_i &= (p_b - q_i)^2, \quad i = 1, 2, 3.
 \end{aligned}
 \tag{1}$$

Of these, five are independent (e.g., the set s, s_1, s_3, t_1, u_3) since they satisfy the linear relations

$$\begin{aligned}
 t_3 &= -s + s_3 - u_3 + M_a^2 + M_b^2 + m_3^2, \\
 u_1 &= -s + s_1 - t_1 + M_a^2 + M_b^2 + m_1^2, \\
 t_2 &= -s_3 - t_1 + u_3 + M_a^2 + m_1^2 + m_2^2, \\
 u_2 &= -s_1 + t_1 - u_3 + M_b^2 + m_2^2 + m_3^2, \\
 s_2 &= s - s_1 - s_3 + m_1^2 + m_2^2 + m_3^2,
 \end{aligned}
 \tag{2}$$

where $M_a, M_b, m_1, m_2,$ and m_3 are the masses of particles $a, b, 1, 2,$ and $3,$ respectively.

The invariants given in (1) can be thought of as the generalization of the Mandelstam variables s, t, u normally considered in two-body reactions. However, if, by analogy with two-body scattering, we try to write a dispersion relation in terms of one of these variables while keeping the other independent ones fixed, it is well known that the production amplitude produces complex singularities in the physical region.³ For example if we were to disperse in the variable $s_1,$ keeping $s, s_3, t_1,$ and u_3 fixed, then, since from Eqs. (2) $s_2 = s - s_1 - s_3 + m_1^2 + m_2^2 + m_3^2,$ we can write

$$\begin{aligned}
 &f(s_1, \dots, s_2, \dots) \\
 &= \frac{1}{\pi} \int_{(m_2+m_3)^2}^{\infty} ds'_1 \frac{\Delta_1 f(s'_1, \dots, s'_2, \dots)}{s'_1 - s_1} \\
 &+ \frac{1}{\pi} \int_{(m_1+m_3)^2}^{\infty} ds'_2 \frac{\Delta_2 f(s'_1, \dots, s'_2, \dots)}{s'_2 - s_2},
 \end{aligned}
 \tag{3}$$

where $\Delta_1 f$ and $\Delta_2 f$ represent the discontinuities across the s_1 and s_2 cuts, respectively. The second integral in Eq. (3) can be rewritten in terms of a left-hand cut in s'_1 as

$$\int_{-\infty}^{\bar{s}_1} \frac{\Delta_2 f(s'_1, \dots, s'_2, \dots)}{s'_1 - s_1} ds'_1.$$

Here $\bar{s}_1 = s - s_3 + m_1^2 + m_2^2 + m_3^2 - (m_1^2 + m_3)^2,$ which in the physical region with $s > (m_1 + m_2 + m_3)^2$ and $s_3 > (m_1 + m_2)^2$ implies $\bar{s}_1 > (m_2 + m_3)^2,$ and the two cuts overlap. Of course it may well be possible to distort one or other of the integral contours away from the real axis to avoid this overlapping, but then it will be necessary to consider the scattering amplitude at complex values of its variables.

A second way in which complex singularities may arise can be seen by considering the triangle graph of Fig. 2.³ Using the reduced variable $z_{\alpha\beta}$ defined by

$$\begin{aligned}
 s_{\alpha\beta} &= (p_\alpha + p_\beta)^2 \\
 &= m_a^2 + m_b^2 + 2m_a m_b z_{\alpha\beta},
 \end{aligned}
 \tag{4}$$

where p_α and p_β are the four-momenta of particles α and $\beta,$ this graph produces a line of singularities given by the equation

$$\det |z_{\alpha\beta}| = 0,
 \tag{5}$$

where $z_{\alpha\beta} = z_{\beta\alpha}, z_{\alpha\alpha} = 1.$

Equation (5) defines the ellipse

$$z_{\lambda\mu}^2 + z_{\lambda\nu}^2 + 2m_x z_{\lambda\mu} z_{\lambda\nu} + m_x^2 - 1 = 0,
 \tag{5'}$$

with

$$m_x^2 = \frac{m^2 - m_\mu^2 - m_\nu^2}{2m_\mu m_\nu},$$

which, as shown in Fig. 3, is tangential to the normal thresholds $z_{\lambda\mu} = 1, z_{\lambda\nu} = 1.$ When $s_{\lambda\mu}$ (and $z_{\lambda\mu}$) is kept fixed and below its normal threshold value, the triangle diagram produces two real singularities given by the intersection of the line $z_{\lambda\mu} = \text{constant}$ with the ellipse (although physical singularities correspond only to that part of the curve AB

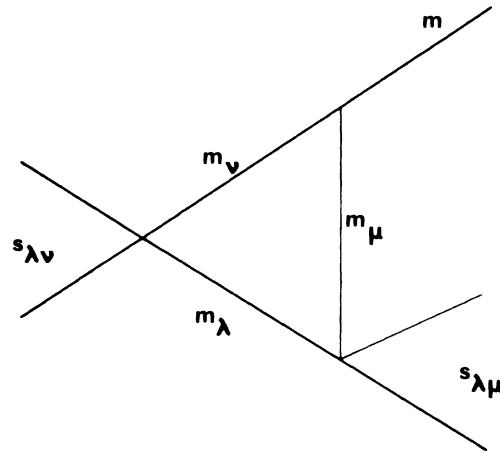


FIG. 2. Triangle diagram.

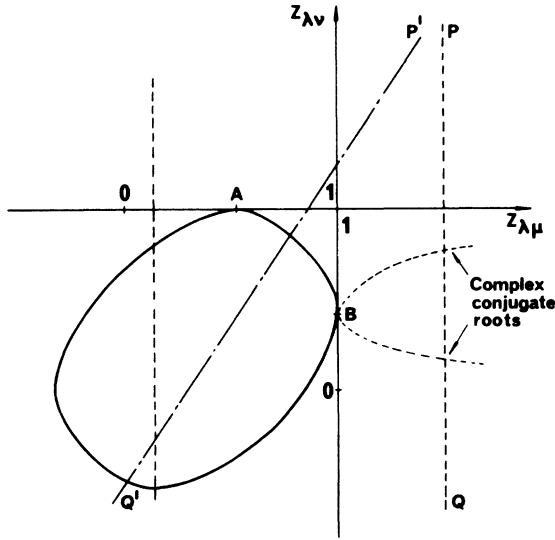


FIG. 3. Singularities of triangle diagram in the $z_{\lambda\mu}$, $z_{\lambda\nu}$ plane.

which lies between the normal thresholds). However, as the value of $z_{\lambda\mu}$ is increased, the line of fixed $z_{\lambda\mu}$ moves to the right in Fig. 3 until it is tangential to the ellipse. At this point the two singularities coincide, and above threshold ($z_{\lambda\mu} > 1$) they become a complex conjugate pair (one physical, one unphysical), the physical one giving rise to a complex branch cut in the physical $s_{\lambda\nu}$ plane. Also, it will generally be possible to draw another triangle graph which depends on one of the variables in Eq. (2), e.g., $t_{\alpha\beta}$ such that $s_{\lambda\nu} = -t_{\alpha\beta} + c$, where c is some fixed quantity of the other invariants. Thus complex singularities will occur in both halves of the $s_{\lambda\nu}$ plane and a dispersion relation in terms of one Lorentz scalar must always involve a complex contour. The situation is clearly going to become even more complicated for higher-order diagrams.

III. PARAMETRIC DISPERSION RELATIONS AND FESR'S

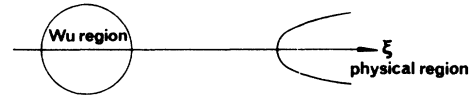
To overcome the problems outlined in the last section let us consider more closely the singularity diagram shown in Fig. 3. So long as $z_{\lambda\mu}$ is below the normal threshold $z_{\lambda\mu} < 1$ there is no difficulty; we have only real singularities given by the intersection of the line PQ with the ellipse. The difficulties arise when $z_{\lambda\mu} > 1$ and PQ lies completely outside the singularity contour so that its points of intersection must necessarily be complex. However, if the dispersion relation is to be of any practical use, at least some of the $z_{\alpha\beta}$ must be above their threshold values at some point.

From Fig. 3 we can see that this can be achieved without introducing complex singularities if we can tilt the line PQ (e.g., onto the line $P'Q'$) so that there is some point on it which lies inside the ellipse and hence $P'Q'$ cuts the ellipse at two real points. In this case both $z_{\lambda\mu}$ and $z_{\lambda\nu}$ vary, rather than keeping one or the other fixed, the variation being parametrized in terms of points on the line $P'Q'$. Of course to eliminate all complex singularities we must consider all possible triangle diagrams and thus generalize the line $P'Q'$ by a line through the whole five-dimensional space of Lorentz scalars. Now instead of having some point inside the $(z_{\lambda\mu}, z_{\lambda\nu})$ ellipse this line must also pass through the intersection of all ellipses arising from all these triangle diagrams. Provided this intersection is free from any singularities arising from higher-order diagrams, we can write a parametric dispersion relation along this line which has only real singularities. Following the work of Wu and Boyling,⁴ who showed that such a singularity-free intersection does indeed exist⁵ to all orders of perturbation theory, Branson, Landshoff, and Taylor⁶ utilized this approach to write a production amplitude dispersion relation for equal-mass particles in the variable ξ , where

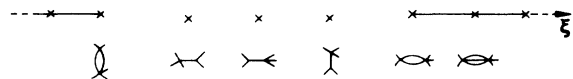
$$\begin{aligned} s &= 9\mu^2 + \xi, \\ s_i &= 4\mu^2 + \frac{1}{3}\xi, \\ t_i &= -\mu^2 - \frac{1}{3}\xi, \\ u_i &= -\mu^2 - \frac{1}{3}\xi, \end{aligned} \quad (6)$$

and μ is the particle mass.

The parametric line characterized by ξ was chosen so that it passed through the singularity-free Wu region and also entered the physical region at the point $\xi=0$, as shown in Fig. 4(a). How-



(a)



(b)

FIG. 4. (a) Diagrammatic representation of the ξ line through the space of Lorentz scalars. (b) Typical singularities of the production amplitude as a function of ξ .

ever, the drawback to this parametrization is that while it lies in physical region for $\xi \geq 0$, the linear relations of Eqs. (6) necessarily mean that it must be in a very unphysical region for negative ξ , i.e., with some momentum transfers tending to $+\infty$. Thus the left-hand singularities, indicated in Fig. 4(b), must involve values of the scattering amplitude at very unphysical points. Furthermore, even for $\xi \rightarrow +\infty$, since all momentum transfers tend to $-\infty$ the asymptotic amplitude cannot simply be parametrized by a few Regge exchanges as one would like if the FESR is to be used to determine the high-energy parameters.

In order to develop a practical approach to dispersion relations for five-point amplitudes we shall adopt a middle course between the fixed-variable and parametric-dispersion relations and write a semiparametric form which leaves certain of the Lorentz scalars fixed while parametrizing others so that we do not encounter complex singularities. Specifically for the process $\pi_a N_b \rightarrow \pi_1 \pi_2 N_3$ we write

$$\begin{aligned} s &= \bar{s} + z[(2\mu + m)^2 - \bar{s}], \\ s_3 &= \bar{s}_3 + z[4\mu^2 - \bar{s}_3], \\ s_1 &= \bar{s}_1, \\ t_1 &= \bar{t}_1, \\ u_3 &= \bar{u}_3, \end{aligned} \quad (7)$$

where m and μ are the masses of the nucleon and pion, respectively.

This form is chosen so that it has the physical-region branch cuts in s and s_3 for $z \geq 1$. Also, with \bar{s} and \bar{s}_3 given by

$$\begin{aligned} \bar{s} &= \frac{1}{2}(m^2 + 2\mu^2 + \bar{s}_1 - \bar{t}_1), \\ \bar{s}_3 &= \frac{1}{2}(3\mu^2 - \bar{t}_1 + \bar{u}_3) \end{aligned} \quad (8)$$

it is a simple matter to show [using Eqs. (1) and (7)] that the crossed process $\bar{\pi}_1 N_b \rightarrow \bar{\pi}_a \pi_2 N_3$ gives rise to physical branch cuts in u_1 and t_2 at $z \leq -1$. However, it must be noted that the point $z = 0$, which we take to be the necessary point inside the Wu region, corresponds to the point $(\bar{s}, \bar{s}_1, \bar{s}_3, \bar{t}_1, \bar{u}_3)$ in our space of invariants. Thus the value of $s_1 = \bar{s}_1$ must always be slightly unphysical, i.e., below the $\pi_2 + N_3$ threshold. This is the price we apparently have to pay to obtain a left-hand-cut contribution which is not determined by extremely unphysical crossed-channel processes (as in the dispersion relation of Ref. 6). In fairness to our approach let us point out that the extrapolation of the physical scattering amplitudes to the point $s_1 = \bar{s}_1$ is less than the extrapolations often performed in two-body FESR's (e.g., where even positive momentum transfers are sometimes considered). In-

deed if we must go outside the physical region, an extrapolation to just below a final-state two-body threshold seems the simplest and least perilous line of approach.

It is also worth mentioning that the reason we have to fix \bar{s}_1 below its threshold value is so that we do not run into the complex singularities arising from a possible triangle diagram with an s_1 final-state interaction. Thus if we can somehow factor out this final-state interaction by defining some suitably modified scattering amplitude, it may be possible to take \bar{s}_1 into the physical region, at least below the first inelastic threshold.

It must be stressed that in any case the parametrization of Eq. (7) we consider in this paper defines a dispersion relation in z which is truly a dispersion relation for particle production amplitudes. We still have to consider final-state effects between $\pi_1 N_3$ and $\pi_1 \pi_2$, and thus it is not equivalent to a quasi-two-body process, even though one final-state subenergy is held fixed.

Figure 5(a) shows diagrammatically the z line defined by Eq. (7) through the space of invariants such that it is inside the Wu region for $z = 0$ and approaches asymptotically the physical regions for $\pi_a N_b \rightarrow \pi_1 \pi_2 N_3$ and the crossed process $\bar{\pi}_1 N_b \rightarrow \bar{\pi}_a \pi_2 N_3$. In Fig. 5(b) we indicate the corresponding cut structure of the production amplitudes $A(s, s_i, t_i, u_i)$ considered as a function of z [i.e., $f(z)$]. It should be noted that asymptotically the kinematics suggests that these amplitudes will be dominated by a few single-Regge-exchange diagrams. The semiparametric dispersion relation or FESR follows by drawing a contour around

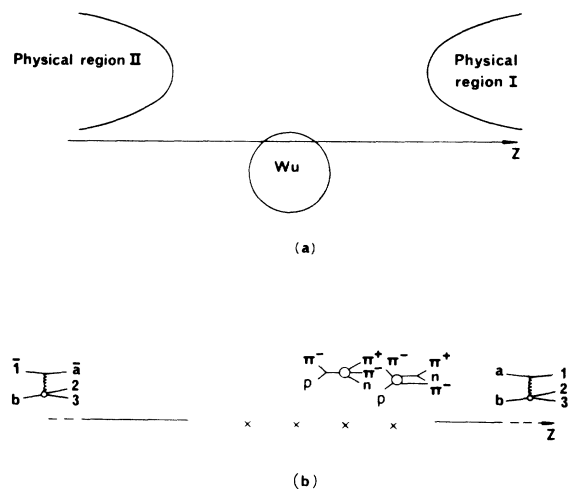


FIG. 5. (a) Diagrammatic representation of the z line through the space of Lorentz scalars. (b) Pole terms and asymptotic limits for the production amplitude as a function of z .

these singularities, closed by two semicircles at infinity and applying Cauchy's theorem. For instance, in terms of the modified amplitude $f(z) - f_{\text{asympt}}(z)$, where $f_{\text{asympt}}(z)$ is the asymptotic amplitude given in terms of the single-Regge-exchange graphs shown in Fig. 5(b), i.e.,⁷

$$f_{\text{asympt}} = \sum_i \gamma_i \frac{1 + \tau e^{-i\pi\alpha_i}}{\sin\pi\alpha_i} (a+bz)^{\alpha_i(t_1)},$$

the production-amplitude FESR can be written as

$$\int_{z_0}^{\Lambda} dz z^m \text{Im} f(z) = \sum_i \int_{z_0}^{\Lambda} dz \tau \gamma_i (a+bz)^{\alpha_i(t_1)} z^m, \quad (9)$$

where it has been assumed that $f(z) \approx f_{\text{asympt}}(z)$ for $|z| \geq \Lambda$, and z_0 is the lower limit of the amplitude singularities in the variable z . Also, $m = 2n$ or $2n+1$, depending on whether f is an odd or even function of z .

In order to utilize Eq. (9) to study the structure of the high-energy amplitudes it is necessary to know in some detail the low-energy production amplitudes. Thus, initially, it is necessary to analyze the low-energy data in terms of a partial-wave expansion. This will be discussed in Sec. V. However, in the next section we shall concentrate on the contribution of the bound-state pole terms to these FESR's.

IV. INVARIANT AMPLITUDES AND BOUND-STATE POLES

In writing the FESR's of Eq. (7) we have assumed that the production amplitude is either symmetric or antisymmetric under the interchange of particles π_a and π_1 . To form amplitudes with these properties, however, we must consider the spin and isospin structure of the process. For instance for $\pi N \rightarrow \pi \pi N$ it is convenient to expand the five-point amplitude into invariants $\bar{A}, \bar{B}, \bar{C}, \bar{D}$ such that

$$\bar{T} = \bar{u}(p_3) \gamma_5 (\bar{A} + \gamma \cdot k^- \bar{B} + \gamma \cdot k^+ \bar{C} + \bar{D} [\gamma \cdot \gamma^+, \gamma \cdot \gamma^-]_-) u(p_b), \quad (10)$$

where γ_5, γ_μ and \bar{u}, u are the usual Dirac matrices and four-spinors, respectively, and $k^- = p_a + q_1$, $k^+ = q_2$, $\gamma^+ = k^- + k^+$, and $\gamma^- = k^- - k^+$. This expansion, which is similar in its general structure to that of Ref. 8, has the property that, provided \bar{T} is symmetric under isospin, then \bar{A} and \bar{C} are symmetric under $\pi_a \leftrightarrow \pi_1$ crossing and \bar{B}, \bar{D} are antisymmetric.

Note that whereas in two-body processes it is possible to work in terms of helicity amplitudes which can be freed from any kinematic singularities, it has been shown by Navelet and Pittet⁹ that

this is not the case for five-point processes. There is always some kinematic singularity in the helicity production amplitudes which can never be factored out completely. It is clearly advantageous therefore to work with the invariant amplitudes which we believe have only dynamical singularities.

Before discussing in detail the analysis of the low-energy amplitudes it is amusing to consider just the nucleon pole terms by themselves. In Fig. 5(b) we have shown four bound-state poles which arise from the nucleon intermediate states

$$\pi N \rightarrow N \rightarrow \pi \pi N$$

and

$$\pi N \rightarrow \pi N \rightarrow \pi N$$

in the direct and crossed channels. These terms can be evaluated in terms of the nucleon propagator, the πNN coupling constant, and the invariant πN amplitudes A, B where

$$T_{\pi N} = \bar{u} [-A + \frac{1}{2} \gamma \cdot (k_1 + k_2) B] u. \quad (11)$$

These pole terms of course should be added to the left-hand side of the sum rule in Eq. (9) and equated to the low-energy integral of the asymptotic form of the amplitude. However, for the particular charge configuration $\pi^- p \rightarrow \pi_1^+ \pi_2^- n_3$ this asymptotic form involves a doubly charged meson exchange, i.e., an exotic exchange which should therefore be strongly suppressed compared to normal Regge exchanges. Thus semilocal duality might suggest that for this particular charge configuration, the discontinuity of the low-energy amplitude, $\text{Im} f(z)$, averages to zero. Taking this reasoning even farther we might naively attempt to equate the two-direct-channel or two-crossed-channel pole terms to zero by themselves. In this case one obtains, for the pole contributions to the antisymmetric amplitudes \bar{B} and \bar{D} , the relations

$$A_{\pi^- n \rightarrow \pi^- n}(z_n) + A_{\pi^- p \rightarrow \pi^- p}(z_p) \approx 0$$

and

$$B_{\pi^- n \rightarrow \pi^- n}(z_n) + B_{\pi^- p \rightarrow \pi^- p}(z_p) \approx 0,$$

respectively, where A and B are the πN invariant amplitudes of Eq. (11) evaluated at the pole positions $z = z_n$ and $z = z_p$. Using typical values for the parameters \bar{s}_1, \bar{t}_1 , and \bar{u}_3 in Eqs. (7) and (8) of 1.15, -0.14, and -0.10 GeV², respectively, the πN amplitudes in Eqs. (12) are to be evaluated at

$$z_n: s_{\pi N} = 1.15 \text{ GeV}^2, t_{\pi N} = 0.033 \text{ GeV}^2,$$

$$z_p: s_{\pi N} = 1.16 \text{ GeV}^2, t_{\pi N} = 0.042 \text{ GeV}^2,$$

where $s_{\pi N}$ and $t_{\pi N}$ are the Mandelstam variables for πN scattering. To a first-order approximation in $t_{\pi N}$ this gives the Weinberg relation for the πN scattering lengths¹⁰

$$2a_{I=3/2} + a_{I=1/2} \approx 0. \quad (13)$$

A similar calculation can be made for the symmetric amplitudes \bar{A} and \bar{C} , but in this case the πN amplitudes are multiplied by factors of z_n , z_p , and certain kinematic quantities which complicate the algebra.

The relation (13) is a very amusing result, coming as it does by imposing the suppression of exotic exchanges on a production amplitude. However, one could argue that this severe form of local duality is not expected to be very well satisfied and Eq. (13) is no more than a happy coincidence. A better test of this result would be to consider a larger region in z than just these pole terms. This we shall do in the following sections.

V. PARTIAL-WAVE ANALYSIS

In the past few years a number of authors have attempted to analyze the low-energy $\pi N \rightarrow \pi_1 \pi_2 N_3$ amplitudes by means of some sort of partial-wave expansions.^{11,12} Unfortunately the data are neither numerous enough nor explicit enough to permit a definitive systematic study of these amplitudes. For instance most of the published data have been in the form of distributions in only one variable, such as an invariant mass or scattering angle, and information on double-differential distributions, even Dalitz plots, is available at only a few widely spaced momenta. This situation is changing rapidly, but until such distributions exist together with polarization measurements with the same sort of statistics that are available for elastic πN scattering we shall have to resort to model making in order to study the low-energy production dynamics.

Because of these limitations on the published analyses we have undertaken our own investigation of the low-energy production data. This is done, not in the hope of improving the analyses at this stage, but so that we have some feeling for the relative importance of various contributions. The model we use is as usual the isobar model. This is very well covered in the literature,^{11,12} and we shall only outline the main features of the particular version employed here. First, a partial-wave expansion is performed on the production helicity amplitudes in the manner proposed by Namyslawski, Razmi, and Roberts (NRR).¹³ This uses the Wick three-particle analysis,¹⁴ which isolates two of the three final-state particles (e.g., π_1 and π_2).

After decomposing this two-body system into states of total and orbital angular momentum j and l in its own c.m. system, we combine each of these states with the third particle (N_3) and again expand into states of total and orbital angular momentum J and L' in the over-all c.m. system. Following NRR, this expansion is performed for each of the two-particle subsystems in the final state, i.e., $\pi_1 \pi_2$, $\pi_1 N_3$, and $\pi_2 N_3$, and each set of states related to each other by means of the Wick recoupling matrices.¹⁴

The resulting partial-wave amplitudes are functions of s , s_i , J , L , L'_i , j_i , and l_i ($i=1,2,3$) as well as isospin. (Here L is the orbital angular momentum of the initial πN state.) The isobar-model assumption is now to write each of these amplitudes as a product of terms, $\mathcal{Q}_{j_i l_i}^{J L L'_i}(s, s_i)$, $\mathcal{P}_{j_i l_i}(s_i)$, and $f_{j_i l_i}(s_i)$, where \mathcal{Q} is the amplitude describing the production of the j_i, l_i isobar and \mathcal{P} and f are respectively the isobar propagator and its decay form factor into the i th two-particle subsystem. In practice we consider only the dominant final-state effects, which we believe are the $I=J = \frac{3}{2} \Delta(1236) \pi N$ resonance and the $I=J=0 \sigma \pi \pi$ resonance. Although recent estimates suggest the σ has a mass comparable with that of the ρ meson, it produces a much larger effect at low subenergies, apparently because of its large width.¹¹⁻¹³ Thus, besides the nucleon-pole terms, the reactions we consider are

$$\begin{aligned} \pi N &\rightarrow \pi_1 \Delta \rightarrow \pi_1(\pi_2 N_3), \\ \pi N &\rightarrow \pi_2 \Delta \rightarrow \pi_2(\pi_1 N_3), \\ \pi N &\rightarrow \sigma N \rightarrow (\pi_1 \pi_2) N_3. \end{aligned} \quad (14)$$

As in the last section, we use the S -wave approximation for the πN amplitudes in calculating the nucleon-pole terms. This is an excellent approximation in determining the pole contributions to the FESR's, as we have already discussed. Moreover, for the analysis of low-energy production data these pole terms represent background contributions arising from three-body effects and the $I=\frac{1}{2} \pi N$ final-state interactions, and hopefully therefore the analysis will be fairly insensitive to their detailed forms.¹¹⁻¹³

For the Δ resonance the parametrization of Ref. 15 for $\mathcal{P}f$ is used, i.e.,

$$\mathcal{P}f_{\Delta} = \frac{ck_{\Delta}}{\sqrt{s_i}} \frac{1}{m_{\Delta}^2 - s_i - im_{\Delta}\Gamma}, \quad (15)$$

where $s_i = s_1$ or s_2 of Eq. (1), k_{Δ} is the momentum of N_3 calculated in the $\pi_1 N_3$ or $\pi_2 N_3$ c.m. system, respectively, and Γ_{Δ} is the total width of the Δ resonance. For the σ resonance, to incorporate its large width and apparent asymmetry, we take

the effective propagator

$$\mathcal{P}f_o = c \left(\frac{s_3}{s_3 - 4\mu^2} \right)^{1/2} e^{i\delta} \sin\delta, \quad (16)$$

where δ is the $I=J=0$ $\pi\pi$ phase shift. In order to account for the energy dependence of the isobar production amplitudes in which the πN initial state of total and orbital angular momenta J and L produces an isobar + particle state with orbital angular momentum L'_i , we insert the threshold factors explicitly and write

$$\mathcal{G}_{j_i i_i}^{J L L'_i}(s, s_i) = p_a^L q_i^{L'_i} \bar{\mathcal{G}}_{j_i i_i}^{J L L'_i}(s, s_i), \quad (17)$$

where p_a and q_i are the momenta of particles a and i in the over-all c.m. system. The reduced production amplitudes $\bar{\mathcal{G}}$ are essentially arbitrary. In most analyses it is approximated by a slowly varying complex function. This may be satisfactory if we only require the relative phase between different isobar contributions. However, in our sum rules we need to know the actual discontinuity of the low-energy production amplitude. To help us in this we make the following observation. Below the three-particle threshold the J, L, L'_i $\pi N \rightarrow \pi\pi N$ partial-wave amplitude has the phase of the corresponding J, L elastic πN amplitude in the variable s . Above the $\pi\pi N$ threshold this need no longer be the case, but so long as we are not too far above, it might still be a good first approximation. So far as we can tell this assumption is compatible with several earlier analyses. (See however, the concluding discussion given by Morgan in Ref. 11.) Also, in the fits described below, although some extra phase dependence was allowed in the partial waves, very reasonable fits could be achieved without it, at least in the incident-pion energy range $T_\pi < 700$ MeV considered.

TABLE I. The isobar contributions to the production partial waves. The scale parameters c have been normalized to 1.0 for the $PP1$ partial wave.

Isospin I	Partial wave	J	L	L'_i	Isobar	Scale parameter
$\frac{1}{2}$	PP1	$\frac{1}{2}$	1	1	Δ	1.0
	DS3	$\frac{3}{2}$	2	0	Δ	0.08
	PS1	$\frac{1}{2}$	1	0	σ	6.7
	DP3	$\frac{3}{2}$	2	1	σ	9.5
	SP1	$\frac{1}{2}$	0	1	σ	1.9
$\frac{3}{2}$	SD1	$\frac{1}{2}$	0	2	Δ	negligible
	DS3	$\frac{1}{2}$	2	0	Δ	0.12
	DD3	$\frac{1}{2}$	2	2	Δ	0.40

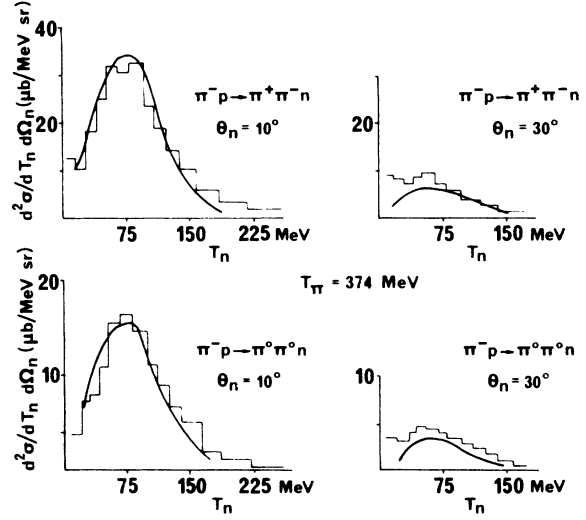


FIG. 6. Double-differential distributions for the processes $\pi^- p \rightarrow \pi^+ \pi^- n$ and $\pi^- p \rightarrow \pi^0 \pi^0 n$ at 374 MeV. Data taken from Ref. 16.

The second approximation we make is to consider only those initial πN partial-wave states which correspond to known low-energy resonances, i.e., S_{11} , P_{11} , and D_{13} . Again this is apparently in agreement with previous analyses.^{11,12} The amplitudes of Eq. (17) were therefore parametrized by suitable Breit-Wigner + background forms which have the appropriate second-sheet resonance poles and πN partial-wave phases.

The remaining arbitrariness is the number of orbital angular momentum states to include for the isobar + particle system. At the energies considered we chose to keep only those waves with

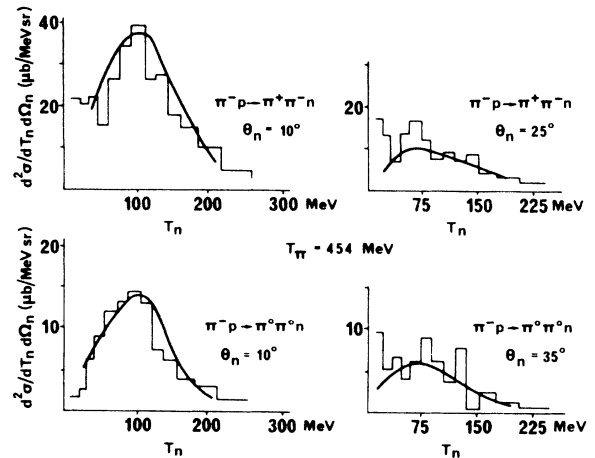


FIG. 7. Double-differential distributions for $\pi^- p \rightarrow \pi^+ \pi^- n$ and $\pi^- p \rightarrow \pi^0 \pi^0 n$ at 454 MeV. Data taken from Ref. 16.

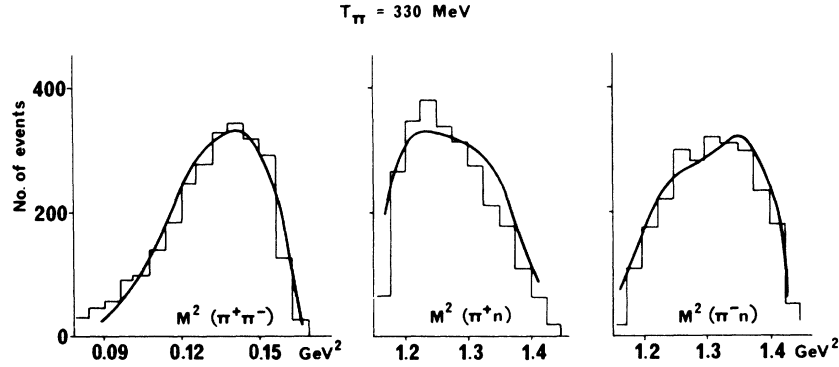


FIG. 8. Invariant (mass)² distributions for the process $\pi^- p \rightarrow \pi^+ \pi^- n$ at 330 MeV. Data taken from Ref. 17.

$L'_i \leq 1$ when the total isospin of the system is $\frac{1}{2}$, and $L'_i \leq 2$ when $I = \frac{3}{2}$. The resulting contributions to the production amplitudes are shown in Table I.

The free parameters in the model are now the constants c in Eqs. (15) and (16), which multiply each of the partial-wave contributions. These were determined by eyeball fits to the experimental distributions presented in Refs. 12 and 16–18, and, as outlined above, were taken to be purely real numbers.

For low incident pion energies $T_\pi \leq 460$ MeV the data of Ref. 16 on $d^2\sigma/dT_N d\cos\theta_N$ were included, where T_N and θ_N are the energy and the scattering angle of the final-state nucleon. These results represent most of the information available on double-differential distributions other than Dalitz plots, and although they are in some disagreement with a similar set produced recently by Muang *et al.*¹⁹ we found that a simultaneous fit to the Dalitz plots of Ref. 17 and the $d^2\sigma/dT_N d\cos\theta_N$ distributions strongly preferred the earlier data. These fits are shown in Figs. 6–10. Since there is some doubt about the mass of the σ resonance, a few different values were tried. It was found that the peaks in $d^2\sigma/dT_N d\cos\theta_N$ for small θ_N (which is es-

entially the “Kurz anomaly”)¹⁶ favored a σ mass above 600 MeV, and for the distributions shown in Figs. 6–10 we have taken $m_\sigma = 800$ MeV.

Having fitted the $\pi^- p \rightarrow \pi^+ \pi^- n$ and $\pi^- p \rightarrow \pi^0 \pi^0 n$ distributions, it is a simple matter to calculate the $\pi^- p \rightarrow \pi^- \pi^0 p$ distributions by the appropriate choice of Clebsch-Gordan coefficients.²⁰ However, in this reaction there is no $I=J=0$ $\pi\pi$ interaction, and the fact that the model curves do not quite fit the data implies we should ideally include some further contribution, probably containing an $I=J=1$ $\pi\pi$ interaction, i.e., a ρ resonance.

For T_π small those partial waves with high orbital angular momentum L'_i are negligible because of the centrifugal barrier. However, as T_π increases these waves can quickly produce a sizeable effect in the distributions. This is clearly seen in those reactions with total isospin $I = \frac{3}{2}$, e.g., the process $\pi^+ p \rightarrow \pi^+ \pi^0 p$. The rapid increase in the $I = \frac{3}{2}$ inelastic πN cross section as T_π increases strongly suggests the presence of states with large L'_i . For this reason we considered a D -wave production of the Δ isobar from both the $S_{33}(1650)$ and $D_{33}(1670)$ $I = \frac{3}{2}$ resonances as well as the s -wave Δ production from the D_{33} state. Typi-

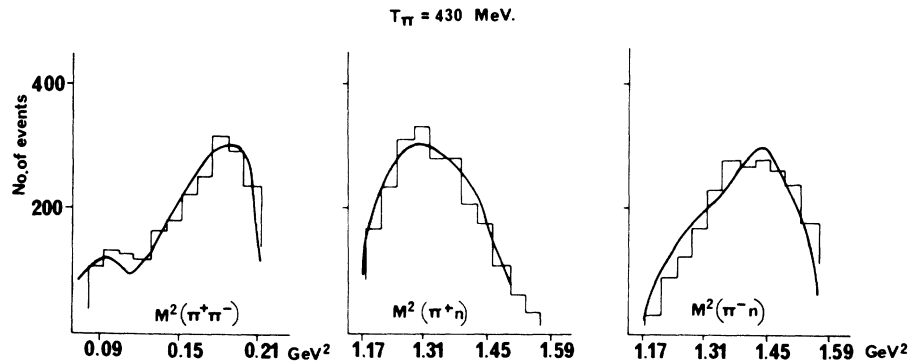


FIG. 9. Invariant (mass)² distribution for $\pi^- p \rightarrow \pi^+ \pi^- n$ at 430 MeV. Data taken from Ref. 17.

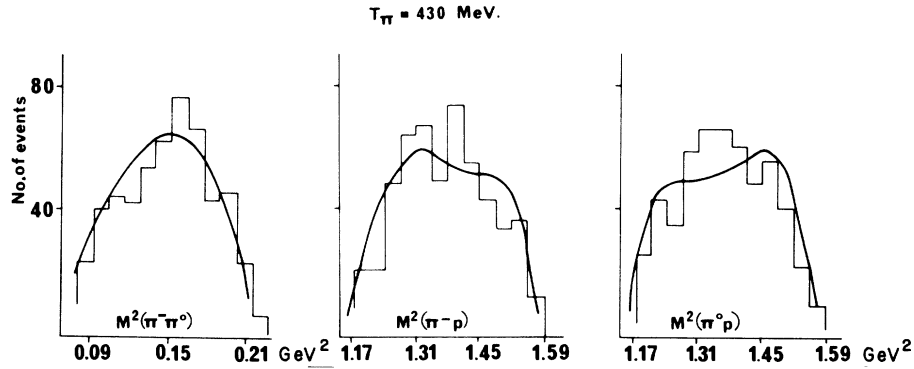


FIG. 10. Invariant (mass)² distribution for the process $\pi^-p \rightarrow \pi^- \pi^0 p$ at 430 MeV. Data taken from Ref. 17.

cal fits to the $\pi^+p \rightarrow \pi^+ \pi^0 p$ distributions with these contributions are shown in Fig. 11.

The $I = \frac{3}{2}$ partial waves, having been determined in this manner, were combined with the $I = \frac{1}{2}$ contributions, which were then varied to fit the π^-p reactions. Besides the energies $T_\pi < 460$ MeV already discussed, data at 495,¹² 558,¹⁸ 565,¹² 604,¹⁸ 646,¹⁸ and 656¹² MeV were also considered. Again we show typical distributions in Figs. 12–14.

To summarize, we have fitted the single-particle production data below $T_\pi \approx 700$ MeV in terms of an isobar model which includes the $\Delta(1236)$ and $\sigma(800)$ final-state effects. These fits are seen to be quite satisfactory except perhaps for the need for some $I = J = 1$ $\pi\pi$ interaction. Presumably it must also be necessary to include some $I = \frac{1}{2}$ final-

state πN interactions in a full analysis of the production amplitudes. Such effects, however, are apparently small at the energies considered here. In this preliminary analysis of the production data we have relied heavily on the results of previous analyses. For instance we used the results of Morgan,¹¹ de Beer *et al.*,¹² and Saxon *et al.*¹⁷ to restrict the range of parameters c considered. The values chosen for the fits shown in Fig. 6–14 are given in Table I. Because of this correspondence with earlier work it is not surprising that the sizes of the πN inelasticity coefficients η_J^f were

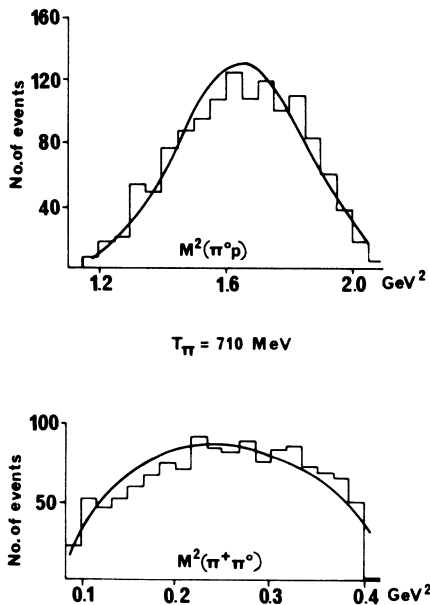


FIG. 11. Invariant (mass)² distributions for the process $\pi^+p \rightarrow \pi^+ \pi^0 p$ at 710 MeV. Data from Ref. 12.

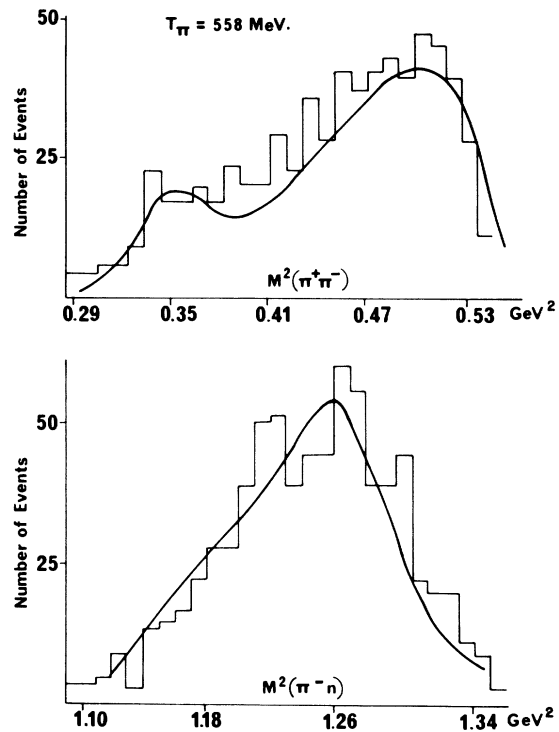


FIG. 12. Invariant (mass)² distributions for $\pi^-p \rightarrow \pi^+ \pi^- n$ at 558 MeV. Data from Ref. 18.

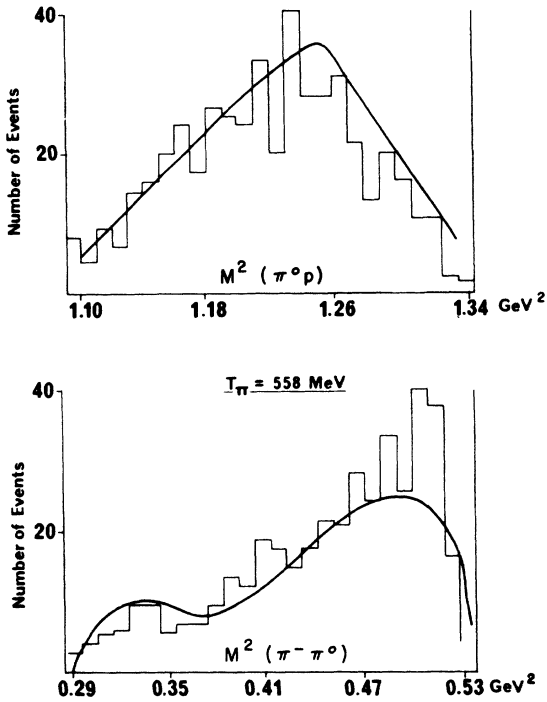


FIG. 13. Invariant (mass)² distributions for $\pi^-p \rightarrow \pi^-\pi^0p$ at 558 MeV. Data from Ref. 18.

obtain are close to those given by de Beer *et al.*¹² and thus are not too different from those given by the elastic πN phase-shift analyses.²¹

The model we use is more restrictive than others

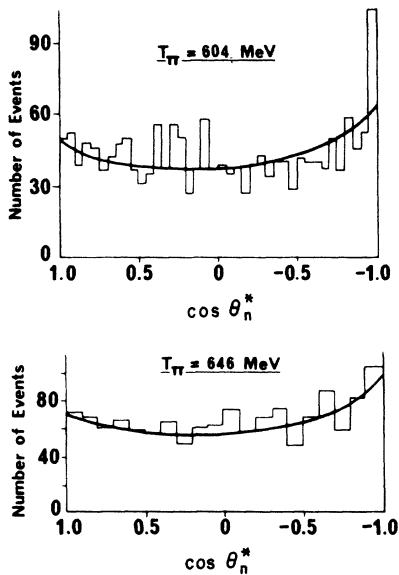


FIG. 14. Nucleon c.m. scattering angle θ_n^* distributions for $\pi^-p \rightarrow \pi^+\pi^-n$ at 604 MeV and 646 MeV.

in the sense that the relative phases between partial-wave contributions are assumed to be known from πN scattering. This rather extreme approximation is found to be acceptable, at least in the fairly small energy range considered.

VI. RESULTS AND DISCUSSION

Having obtained the fit to the data discussed in the last section, we can now use the model to describe the low-energy helicity production amplitudes. These in turn can be related to the invariant amplitudes $\bar{A}, \bar{B}, \bar{C}, \bar{D}$ of Eq. (10) and extrapolated to lie on the z line through the space of Lorentz scalars given by Eq. (7). In practice we find in Eq. (10) that the coefficients multiplying the amplitude \bar{C} are relatively small on this line and thus large variations in \bar{C} produce little effect on the helicity amplitudes. To simplify the preliminary investigation therefore we neglect \bar{C} . Also, after solving for the remaining amplitudes \bar{A}, \bar{B} , and \bar{D} we find that \bar{D} is at least an order of magnitude smaller than \bar{A} and \bar{B} . Thus in view of the approximate nature of both the model and the data we shall not discuss this amplitude further.

The discontinuities in the variable z of the invariant \bar{A} and \bar{B} amplitudes are shown in Fig. 15 for the particularly interesting charge state $\pi^-p \rightarrow \pi_1^+\pi_2^-n$. Here the z -line parameters are²²

$$\bar{s}_1 = 1.15 \text{ GeV}^2,$$

$$\bar{t}_1 = -0.14 \text{ GeV}^2,$$

$$\bar{u}_3 = -0.10 \text{ GeV}^2,$$

and since this reaction is crossing-symmetric in the charge indices the symmetric amplitude \bar{A} has been multiplied by z to obtain the integrand of the first-order FESR. As discussed in Sec. IV, the high-energy (large- $|z|$) limit of this particular reaction corresponds to an exotic double charge exchange, and experience with two-body FESR's suggests that the right-hand side of the sum rules in Eq. (9) should be negligibly small. Equating this to the left-hand side of Eq. (9) we might expect therefore that the integrand should oscillate about zero. As we see in Fig. 15 this is indeed the case.

Let us now consider the particular combination of charge states $\pi^-p \rightarrow \pi_1^-\pi_2^+n + \pi^+p \rightarrow \pi^+\pi^+n$. This is also charge-crossing-symmetric, but unlike the previous case it should be controlled at high energies by well-known Regge exchanges P, P' , etc. However, so far as the low-energy production amplitudes are concerned this is dominated by the reaction $\pi^-p \rightarrow \pi_1^-\pi_2^+n$ since the $I = \frac{3}{2}$ amplitude $\pi^+p \rightarrow \pi^+\pi^+n$ is relatively small ($\leq 10\%$ of the total).¹⁸

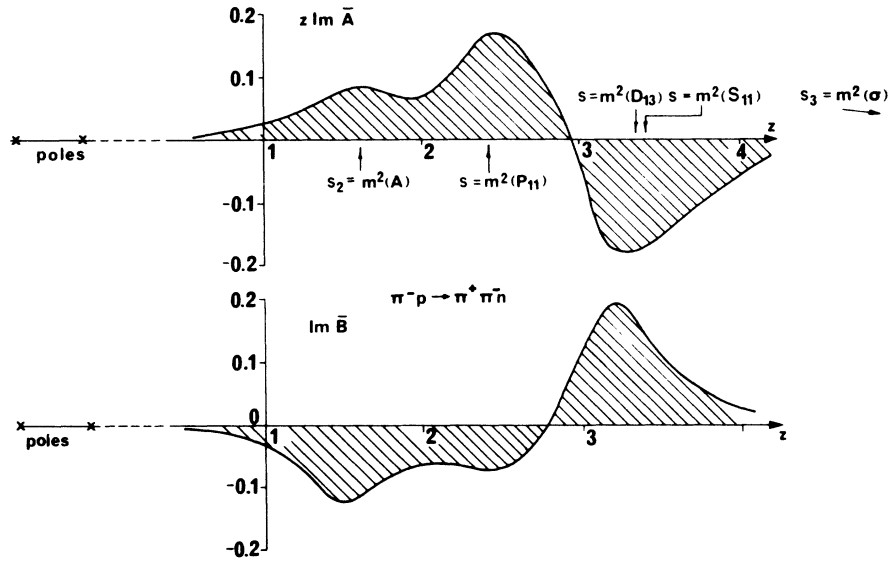


FIG. 15. Integrands of the FESR's of Eq. (9) for the process $\pi^- p \rightarrow \pi_1^+ \pi_2^- n_3$. The positions of the various resonance poles in the model are indicated. Although the σ resonance is above the range of s_3 considered, its effect is still sizeable because of its large width.

Thus it differs from the $\pi^- p \rightarrow \pi_1^+ \pi_2^- n$ reaction essentially only by the interchange of the π^+ and π^- , which is trivially described by a change of Clebsch-Gordan coefficients multiplying the various isospin states. Nevertheless, as can be seen in Fig. 16, this change is sufficient to alter the invariant amplitudes so that their imaginary parts no longer average to zero. Using a cutoff $z = \Lambda$ which corresponds to the midpoint between the second and third s -channel resonance regions, i.e., $s \approx 2.6$ GeV, the corresponding values of

these FESR's are given in Table II. Here we have also included for comparison a further crossing-symmetric isospin combination corresponding to the reaction $\pi^0 p \rightarrow \pi^0 n^0 p$.

Although we should not place much reliance on the results at this stage, it is interesting to use the FESR's to try to calculate the high-energy parameters from the low-energy amplitudes. For instance the values given in Table II can be equated to the integrals of the Regge contributions on the right-hand side of Eq. (9). However, to do this

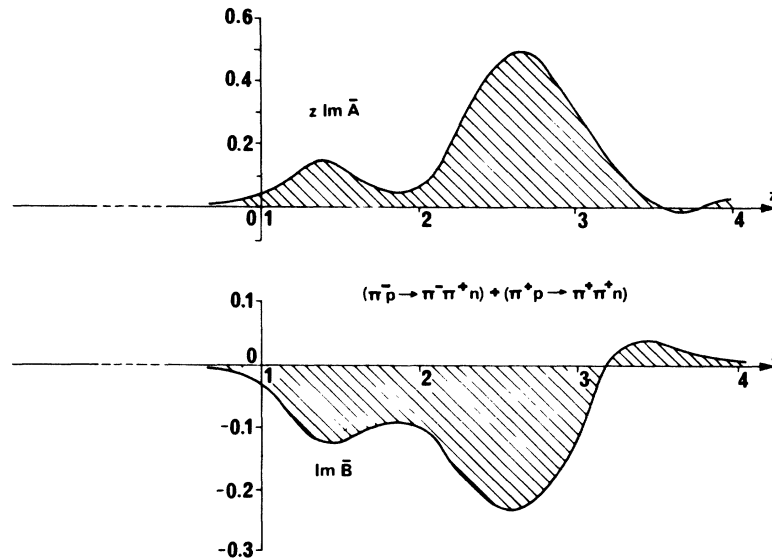


FIG. 16. Integrands of the FESR's for the charge combination $(\pi^- p \rightarrow \pi_1^- \pi_2^+ n_3) + (\pi^+ p \rightarrow \pi^+ \pi^+ n)$.

TABLE II. Evaluation of the left-hand side of Eq. (9) for various charge processes.

Process	FESR values	
	$\int^{\Lambda} z A dz$	$\int^{\Lambda} B dz$
$\pi^- p \rightarrow \pi_1^+ \pi_2^- n_3$	0.41	0.009
$\pi^- p \rightarrow \pi_1^- \pi_2^+ n_3$	2.34	-1.31
$\pi^0 p \rightarrow \pi^0 \pi^0 p$	11.92	-3.07

we would need to know the absolute normalization of both the low- and high-energy amplitudes. A less restrictive calculation is to take a slightly different z line through the space of Lorentz scalars, i.e., with different parameters \bar{s}_1, \bar{u}_3 . Then provided we keep t_1 and the cutoff Λ fixed and assume that the Regge residue function γ_1 is slowly varying we can relate the ratio of left-hand-side values of Eq. (9) to the right-hand-side ratio

$$\frac{\int_{z_0}^{\Lambda} z^m (a + bz)^{\alpha_{\text{eff}}(t_1) - n}}{\int_{z_0}^{\Lambda} z^m (a' + b'z)^{\alpha_{\text{eff}}(t_1) - n}}, \quad (18)$$

where $n=0$ for the A amplitude and $n=1$ for the B amplitude.

This second z line we consider is given by the parameters

$$\begin{aligned} \bar{s}_1 &= 1.15 \text{ GeV}^2, \\ \bar{t}_1 &= -0.14 \text{ GeV}^2, \\ \bar{u}_3 &= -0.11 \text{ GeV}^2. \end{aligned}$$

In order to evaluate the ratio in (18) we have to identify the Regge energy variable $a + bz$. Since u_3 is also kept small, the variable we choose is $s_3 - t_2$, which is crossing-symmetric under the interchange of π_a, π_1 . Equating (18) to the corresponding left-hand-side ratios we obtain the values of the effective Regge trajectories $\alpha_{\text{eff}}(\bar{t}_1)$ shown in the first line of Table III. Considering the approximate nature of the model and the low value of the cutoff these are eminently reasonable values. To check that these results are more than a happy accident some of the scale parameters c in the model were allowed to vary. It was found that so long as the resulting production amplitude still gave reasonable fits to the low-energy data the value of $\alpha_{\text{eff}}(\bar{t}_1)$ remained quite acceptable. A selection of these results are given in Table III. When a similar analysis was performed for the reaction $\pi^- p \rightarrow \pi_1^+ \pi_2^- n$ the values of α_{eff} ranged from -5 to $+5$. However, this is hardly surprising, since the calculation involves the ratio of small quantities, which is very sensitive to small changes in the amplitudes. Hence this is not a

reliable way to determine the effective trajectory for exotic exchanges.

It is perhaps relevant to make here one or two comments about the values of α_{eff} shown in Table III. With some imagination and careful selection one might suggest that the results for \bar{B} look somewhat like the Pomeranchuk trajectory $\alpha_P \lesssim 1.0$ and that those for \bar{A} look like $\alpha_{P'} \lesssim 0.5$. This would be a very interesting result since over the z range considered in Eq. (18) the s -channel helicity-non-flip amplitudes make up at least 65% of the \bar{B} amplitude, while they contribute at most 20% to \bar{A} . Thus we might conclude that these results are consistent with the Pomeranchon-conserving s -channel helicity. However, if this is so we must understand how the Pomeranchon has been produced from a resonance-type model, since it is currently believed that the Pomeranchon is made up of background effects. To answer this let us note that although only resonating partial waves have been considered both for the production and decay amplitudes, these contributions have been parameterized so that they give the appropriate two-body phase shift. Thus some background has already been included. Furthermore, we have attempted to fit all the data by our model, and hence the background arising from nonresonating partial waves has also apparently been well approximated by our fit. It may not be too surprising therefore that the FESR's are trying to give us information about the P as well as the P' trajectories. It would be interesting to see if the Pomeranchon contribution could be confirmed by the explicit addition of nonresonating effects in our model, e.g., by using effective propagators as in Eq. (16), to introduce the relevant phase shifts. However, there is already some freedom in our fits, as can be seen from the results in Table III, and at present we are unable to prefer one set of results over another. Hopefully this freedom can be eliminated to some extent by the inclusion of high-statistics data, which are now becoming available.

TABLE III. The effective trajectory calculated from the \bar{A} and \bar{B} production amplitudes for various values of the scale parameters.

Scale parameter c				$\alpha_{\text{eff}}(t_1)$			
				$(\pi^- p \rightarrow \pi^- \pi^+ n)$ $+ (\pi^+ p \rightarrow \pi^+ \pi^+ n)$		$\pi^0 p \rightarrow \pi^0 \pi^0 p$	
DS3	PS1	DP3	SP1	\bar{A}	\bar{B}	\bar{A}	\bar{B}
0.08	6.7	9.5	1.9	0.64	0.83	0.41	0.66
0.08	6.3	9.1	1.9	0.49	0.87	0.45	0.23
0.08	5.9	8.7	1.9	0.42	0.90	1.10	1.3
0.01	9.5	8.7	0.5	0.55	0.65	0.40	0.49

This is perhaps as far as we can go in the use of our production sum rules at this stage. There seems little point in taking further z lines through the space of Lorentz scalars with different values of \bar{l}_1 to determine the slope and intercept of α_{eff} . Clearly more work has to be done in understanding the low-energy amplitudes before we can make any definitive statements regarding their evaluation of the high-energy behavior. However, we have already come a long way. The results shown in Figs. 15 and 16 and Table III indicate that there is clearly some connection between the interrelation of various low-energy contributions and the asymptotic amplitudes. Indeed they are encouraging enough for us to contemplate a much fuller partial-wave analysis of the single-particle production data. Of course, one of the drawbacks of such an analysis is that we require the over-all phase of the production amplitudes, not just the relative phases between different contributions. However, even here the FESR's can be very helpful. By using one of these sum rules (preferably that corresponding to exotic exchanges) we should be able to obtain a consistency condition on the partial-wave solutions. Furthermore, the choice of the isobar model itself may also be severely tested by considering its effect in a subtracted z -parameter dispersion relation. This should provide a much more sensitive test of the model than usual fits to the data allow, since one is looking directly at the production amplitudes rather than at integrated products of them. In particular the dispersion relation is based on the analyticity of the production amplitude given by considering all orders of Feynman diagrams. Thus it can incorporate effects arising from the triangle diagrams of Sec.

II, which are ignored in isobar-model calculations.

In conclusion, we believe the dispersion-relation techniques outlined in this paper represent a very necessary step in understanding production dynamics. In the form of FESR's discussed here, they allow a much more detailed examination of the production data than the usual dual-model analyses. It is a simple matter to show that such models must satisfy these FESR's but, of course, they are by no means the only solution to them. The FESR's can accommodate various features which are extremely difficult to fit into the dual-model scheme. The most obvious example of these is the Pom-eranchon. In two-body scattering, Harari and Freund have conjectured that this is dual to the nonresonating background.²³ Such a hypothesis is difficult to test, since it is often hard to distinguish background from true resonance effects. In production reactions the situation is even worse because in any subenergy channel there will be background effects arising from the overlap of resonances in other subenergies. Nevertheless if such effects are ever to be understood it is clear that it must come about through sum-rule calculations rather than model fits.

ACKNOWLEDGMENTS

The author should like to thank Professor A. Donnachie, Dr. M. Vaughn, and Dr. R. K. P. Zia for their interest and encouragement in this work. He is also indebted to Dr. R. Alvarez Estrada and Dr. H. Navelet for helpful discussions on the analyticity and helicity structure of the five-point amplitudes.

¹R. Dolen, D. Horn, and C. Schmid, Phys. Rev. 166, 1768 (1968).

²See, for instance, E. L. Berger, Argonne National Lab. Report No. ANL/HEP 711 (unpublished), and in *Phenomenology in Particle Physics, 1971*, proceedings of the conference held at Caltech, 1971, edited by C. B. Chiu, G. C. Fox, and A. J. G. Hey (Caltech, Pasadena, 1971).

³P. V. Landshoff and S. B. Treiman, Nuovo Cimento 19, 1249 (1961).

⁴T. T. Wu, Phys. Rev. 123, 678 (1961); J. D. Boyling, Ann. Phys. (N.Y.) 25, 249 (1963).

⁵The definition of this singularity-free region is not simple, particularly for unequal-mass particles. For the present discussion we only require that it in fact exist in certain physical cases, e.g., $\pi N \rightarrow \pi\pi N$, and that it be disjoint from the physical regions.

⁶D. Branson, P. V. Landshoff, and J. C. Taylor, Phys.

Rev. 132, 902 (1963).

⁷It is not clear *a priori* which is the appropriate energy variable s , s_3 etc. to use in the extrapolation to finite z . Hence for the moment we shall cover all cases by using $a + bz$.

⁸P. Moussa and H. Stern, Saclay report, 1970 (unpublished).

⁹H. Navelet and E. Pittet, Nuovo Cimento 7A, 185 (1972).

¹⁰S. Weinberg, Phys. Rev. Letters 17, 616 (1966).

¹¹S. Bergia, F. Bonsignori, and A. Stanghellini, Nuovo Cimento 16, 1073 (1960); S. J. Lindenbaum and R. Sternheimer, Phys. Rev. 123, 333 (1961); M. Olsson and G. B. Yodh, *ibid.* 145, 1309 (1966); 145, 1327 (1966); Phys. Rev. Letters 10, 353 (1963); J. D. Jackson, Nuovo Cimento 34, 1644 (1964); K. Gottfried and J. D. Jackson, *ibid.* 33, 309 (1964); D. Morgan, Phys. Rev. 166, 1731 (1968).

- ¹²M. de Beer *et al.*, Nucl. Phys. B12, 599 (1969).
- ¹³J. M. Namyslowski, M. S. K. Razmi, and R. G. Roberts, Phys. Rev. 157, 1328 (1967). Note the corrections to this paper given in Ref. 15.
- ¹⁴G. C. Wick, Ann. Phys. (N.Y.) 18, 65 (1962).
- ¹⁵J. C. Botke, Nucl. Phys. B23, 253 (1970).
- ¹⁶B. C. Barish, R. J. Kurz, V. Perez-Mendez, and J. Solomon, Phys. Rev. 135, B416 (1964), and references therein.
- ¹⁷D. H. Saxon, D. Phil. thesis, Oxford, 1969 (unpublished); D. H. Saxon, J. H. Mulvey, and W. Chinowsky, Oxford Univ. Report No. 3/70, 1970 (unpublished).
- ¹⁸R. A. Burnstein *et al.*, Phys. Rev. 137, B1044 (1965); C. N. Vittitoe *et al.*, *ibid.* 135, B232 (1964); J. D. Oliver, I. Nadelhaft, and G. B. Yodh, *ibid.* 147, 932 (1966).
- ¹⁹T. Muang *et al.*, Univ. of California San Diego report 1970 (unpublished).
- ²⁰For a discussion of the isospin analysis of five-point amplitudes see Ref. 11 or S. Humble, Daresbury Lecture Note Series No. 7, 1971 (unpublished).
- ²¹P. Bareyre, C. Bricman, and G. Villet, Phys. Rev. 165, 1730 (1968); A. Donnachie, R. G. Kirsopp, and C. Lovelace, Phys. Letters 26B, 161 (1968).
- ²²These parameters were chosen so that the extrapolation outside the physical region is kept as small as possible.
- ²³H. Harari, Phys. Rev. Letters 20, 1395 (1968).